sensors

MDPI

Article

A Novel Thiophene-Based Fluorescent Chemosensor for the Detection of Zn^{2+} and CN^{-}: Imaging Applications in Live Cells and Zebrafish

Min Seon Kim [1], Dongju Yun [1], Ju Byeong Chae [1], Haeri So [1], Hyojin Lee [2], Ki-Tae Kim [2,*], Mingeun Kim [3], Mi Hee Lim [3] and Cheal Kim [1,*]

1 Department of Fine Chemistry, Seoul National University of Science and Technology, Seoul 01187, Korea; dltmf2303@naver.com (M.S.K.); juju9593@hanmail.net (D.Y.); ch920812@naver.com (J.B.C.); gofl0988@naver.com (H.S.)

2 Department of Environmental Engineering, Seoul National University of Science and Technology, Seoul 01187, Korea.; hyojin_lee@seoultech.ac.kr

3 Department of Chemistry, Korea Advanced Institute of Science and Technology, Daejeon 34140, Korea; mingeun@unist.ac.kr (M.K.); miheelim@kaist.ac.kr (M.H.L.)

* Correspondence: ktkim@seoultech.ac.kr (K.-T.K.); chealkim@snut.ac.kr (C.K.); Tel.: +82-2-970-6642 (K.-T.K.); +82-2-971-6680 (C.K.); Fax: +82-2-971-9147 (C.K.)

Received: 25 October 2019; Accepted: 9 December 2019; Published: 11 December 2019

Abstract: A novel fluorescent turn-on chemosensor **DHADC** ((E)-3-((4-(diethylamino)-2-hydroxybenzylidene)amino)-2,3-dihydrothiophene-2-carboxamide) has been developed and used to detect Zn^{2+} and CN^{-}. Compound **DHADC** displayed a notable fluorescence increase with Zn^{2+}. The limit of detection (2.55 ± 0.05 μM) for zinc ion was far below the standard (76 μM) of the WHO (World Health Organization). In particular, compound **DHADC** could be applied to determine Zn^{2+} in real samples, and to image Zn^{2+} in both HeLa cells and zebrafish. Additionally, **DHADC** could detect CN^{-} through a fluorescence enhancement with little inhibition with the existence of other types of anions. The detection processes of compound **DHADC** for Zn^{2+} and CN^{-} were demonstrated with various analytical methods like Job plots, ^{1}H NMR titrations, and ESI-Mass analyses.

Keywords: fluorescence chemosensor; zinc; cyanide; living cell; zebrafish

1. Introduction

The design of chemosensors with high selectivity and sensitivity has received great interest because they can recognize environmentally and biologically crucial metal ions and anions [1,2]. Among these ions, zinc ion is not only one of the essential metal ions in the human body, but is also the second richest transition metal ion [3,4]. It has large roles at catalytic sites of myriad Zn^{2+}-containing metalloenzymes and in DNA-binding proteins [5,6]. Meanwhile, an uncontrolled zinc concentration in the body creates a wide variety of troubles like epilepsy, Parkinson disease, and ischemic stroke [7]. Hence, it is of great significance to design chemosensors for the selective sensing of Zn^{2+} in biological systems [8–11].

Recently, anions have attracted notable interest, owing to their various roles in clinical, environmental, and biological applications [12–14]. In particular, cyanide has been extensively used in numerous territories like synthetic fiber, gold mining, resin industries, and metallurgy [15–18]. Thus, the voluminous usage of cyanide is ineludible, and numerous industries yield about 140 k tons/year of cyanide [19–21]. However, cyanide acts as a strong poison. Its toxicity induces the susceptibility of binding to iron ion in metalloprotein cytochrome oxidase, blocking the electron transfer chain in mitochondria [22–24]. Moreover, high levels of cyanide can cause convulsions,

vomiting, loss of consciousness, and ultimately death [25,26]. Thus, it is essential to develop an effective sensing tool to recognize the cyanide level in living organisms and environments [27,28].

Among various analytical methods, a fluorescent method has attracted much attention due to its high selectivity, simplicity, and bioimaging ability [29–32]. Until now, a few fluorescence chemosensors for detecting both Zn^{2+} and CN^- were developed, but they are still rare. In addition, zinc fluorescent chemosensors for bioimaging in living cells and zebrafish are very rare (Table S1) [33–39]. Therefore, the development of fluorescent chemosensors with high selectivity and bioimaging ability in both living cells and zebrafish is needed.

Thiophene derivatives have been extensively utilized as a fluorescence signaling promoter to anions, organic acids, and metal ions [40,41]. Moreover, 4-diethylaminosalicylaldehyde moiety is an outstanding fluorophore that has a water-soluble electron-donor property [42,43]. Thus, we combined the two functional groups to design a novel and practical fluorescent sensor, which is expected to sense a particular analyte through a unique fluorescent property with bioimaging ability in both living cells and zebrafish.

Here, we demonstrate a novel and stable fluorescent chemosensor **DHADC,** comprised of 3-aminothiophene-2-carboxamide as a fluorescence-signaling group and 4-diethylaminosalicylaldehyde as an electron-donating group (Scheme 1). Chemosensor **DHADC** detected both Zn^{2+} and CN^- by fluorescent turn-on. To interpret their detecting systems, diverse analytical investigations like ESI-mass analyses, ^{1}H NMR titrations, and Job plots were carried out.

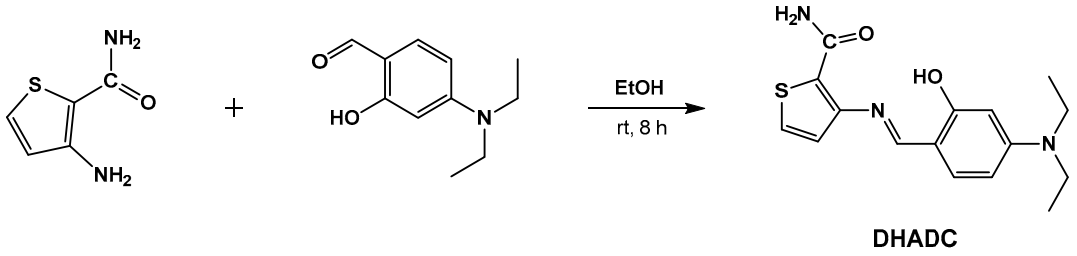

Scheme 1. Synthesis procedure of **DHADC**.

2. Experimental

2.1. Reagents and Equipments

Chemicals were purchased from Sigma–Aldrich. A Varian spectrometer was used to obtain ^{13}C (100 MHz) and ^{1}H NMR (400 MHz) spectra. Fluorescence emission and UV-visible absorption spectra were recorded with Perkin Elmer spectrometers. ESI-MS data were obtained by a Thermo quadrupole ion trap. Fluorescence imaging in zebrafish and cells was obtained by a using fluorescence microscope (MDG36, Leica and EVOS FL, Thermo Fisher Scientific). * Caution for the use of cyanide: Skin, respiratory, and eye protection is required.

*2.2. Synthesis of Sensor **DHADC***
((E)-3-((4-(diethylamino)-2-hydroxybenzylidene)amino)-2,3-dihydrothiophene-2-carboxamide)

3-Aminothiophene-2-carboxamide (1.1 mmol, 160 mg) and 4-diethylaminosalicylaldehyde (1 mmol, 200 mg) was dissolved in 12.0 mL of ethanol and blended for 8 h at 20 °C. The deep orange powder was given by filtration and purified with ether. The yield: 72 % (230 mg); ^{1}H NMR: 11.42 (s, 1H), 8.77 (s, 1H), 8.01 (s, 1H), 7.72 (d, J = 5.2 Hz, 1H), 7.62 (s, 1H), 7.50 (d, J = 8.8 Hz, 1H), 7.38 (d, J = 5.2 Hz, 1H), 6.36 (d, J = 8.8 Hz, 1H), 6.13 (s, 1H), 3.38 (m, 4H), 1.13 (t, J = 5.6 Hz, 6H); and ^{13}C NMR: 163.74, 162.29, 159.94, 159.93, 152.67, 149.72, 132.52, 129.91, 120.31, 109.47, 105.12, 97.26, 44.50, and 12.99. ESI-MS for [**DHADC** ($C_{16}H_{19}N_3O_2S$) + H^+]$^+$: calcd, 318.13 (*m/z*); found, 318.21 (*m/z*).

2.3. Fluorescence Titrations

1.0 mL of DMSO solvent was used to prepare a stock **DHADC** solution (1×10^{-2} mmol, 3.2 mg) and 3.0 μL of the stock solution was diluted to 2.997 mL bis-tris buffer (1×10^{-2} M, pH 7.0). 3–45 μL of zinc ion stock solution (0.1 M) dissolved in bis-tris buffer were added to **DHADC** (3.0 mL, 1×10^{-2} mM). After blending them for 20 sec, fluorescence spectra were obtained. Both **DHADC** and **DHADC**-Zn^{2+} showed no decomposition for 7 h in buffer condition.

For CN^-, 1.0 mL of DMSO solvent was used to prepare a stock **DHADC** solution (1×10^{-2} mmol, 3.2 mg) and its eventual concentration (1×10^{-2} mM) was given by adding 3 μL of stock **DHADC** solution (1×10^{-2} M) into 2.996 mL MeCN. MeCN (1 mL) was employed to dissolve TEACN (tetraethylammonium cyanide, 33.1 mg (0.2 mmol)). 1.5–18 μL of cyanide (200 mM) were added to the compound **DHADC** (3.0 mL, 1×10^{-2} mM). After mixing them for 20 sec, fluorescence spectra were obtained. The titrations for Zn^{2+} and CN^- were conducted three times for the average.

2.4. UV-vis Titrations

3 μL of a stock **DHADC** solution (1×10^{-2} M) was transferred in fluorescent cell containing 2.997 mL bis-tris buffer. 6–42 μL of a zinc ion stock solution (0.1 M) in bis-tris buffer were added to the compound **DHADC** (3.0 mL, 1×10^{-2} mM). UV-vis spectra were obtained after blending them for 20 s.

For CN^-, 3 μL of a stock **DHADC** solution (1×10^{-2} M) was added into 2.997 mL MeCN. 1.5–15 μL of this CN^- (0.2 M) in MeCN were added to the compound **DHADC** (3.0 mL, 1×10^{-2} mM). UV-vis spectra were obtained after blending them for 20 s.

2.5. Job Plots

350 μL of a stock **DHADC** solution (1×10^{-2} M) in DMSO was diluted to 49.65 mL bis-tris buffer for producing 0.07 mM. 0.3–2.7 mL of the diluted compound **DHADC** was added to fluorescent cells, respectively. 35 μL of a Zn^{2+} ion stock (1×10^{-1} M) solution in bis-tris buffer was diluted to 49.97 mL bis-tris buffer. 2.7–0.3 mL of the diluted zinc ion was added to each **DHADC** in fluorescent cells. The total volume of each fluorescent cell was 3.0 mL. Fluorescence spectra were obtained after blending them for 20 s.

For CN^-, 0.6 mL of a stock **DHADC** (1×10^{-2} M) solution in DMSO was diluted to 29.4 mL MeCN/bis-tris buffer (95:5; v/v) to produce 2×10^{-2} M. 0.3–2.7 mL of the diluted compound **DHADC** was added to fluorescence cells, respectively. 30 μL of a CN^- stock solution (0.2 M) in MeCN was diluted to 29.97 mL MeCN/bis-tris buffer solution (95:5). 2.7–0.3 mL of the diluted cyanide was added to each **DHADC** in fluorescent cells. The total volume of each fluorescent cell was 3.0 mL. UV-visible spectra were obtained after blending them for 20 s.

2.6. Competition Tests

1×10^{-2} mmol of $Al(NO_3)_3$ or $NaNO_3$ or $Fe(ClO_4)_2$ or $In(NO_3)_3$ or KNO_3 or $Ga(NO_3)_3$ or $M(NO_3)_2$ (M = Ni, Pb, Ca, Mg, Cu, Mn, Co, and Cd), or $Fe(NO_3)_3$ or $Cr(NO_3)_3$ was separately dissolved in 1.0 mL of bis-tris buffer. 42 μL of each metal ion (1×10^{-1} M) was added into 3.0 mL bis-tris buffer to produce 140 equiv. Following the addition of 42.0 μL of a zinc ion stock solution (0.1 M), 3.0 μL of a stock **DHADC** solution (1×10^{-2} M) was added into the fluorescent cells containing each metal ion. Fluorescence spectra were obtained after blending them for 20 s.

For CN^-, 0.2 mmol of $NaNO_2$, tetraethylammonium salts of F^-, I^- Cl^-, and Br^-, Na_2S and tetrabutylammonium salts of N_3^-, $H_2PO_4^-$, OAc^-, SCN^-, and BzO^- was separately dissolved in 1.0 mL of bis-tris buffer. 15 μL (2×10^{-1} M) of each anion was put into 3.0 mL MeCN/bis-tris buffer (95:5) to afford 100 equiv. Following the addition of 15 μL of TEACN solution (200 mM), 2 μL (1×10^{-2} M) of compound **DHADC** was added into the fluorescent cells containing each anion. Fluorescence spectra were obtained after blending them for 20 s.

2.7. ^1H NMR Titrations

DMSO-d_6 (2.8 mL) was used to dissolve compound **DHADC** (6.4 mg and 0.02 mmol) and 700 μL of **DHADC** was transferred to three NMR tubes, respectively. 0, 0.5, and 1 equiv of Zn^{2+} dissolved. in 1.2 mL of DMSO-d_6 solvent were added to each compound **DHADC**. ^{1}H NMR spectra were obtained after blending them for 20 s.

For CN^-, DMSO-d_6 (2.8 mL) was used to dissolve **DHADC** (6.4 mg, 0.02 mmol) and 700 μL of **DHADC** was transferred to four NMR tubes, respectively. 0, 0.5, 1, and 2 equiv of TEACN dissolved in 2.4 mL of DMSO-d_6 solvent were added to each compound **DHADC**. ^{1}H NMR spectra were obtained after blending them for 20 s.

2.8. Quantum Yields

The quantum yields of **DHADC**, **DHADC**-Zn^{2+} and **DHADC**-CN^- were determined with fluorescein (Φ_F = 0.92) in basic ethanol as a reference fluorophore. By using calibration curves of fluorescein and their absorption spectrum, the concentrations of fluorescein corresponding to each **DHADC**, **DHADC**-Zn^{2+}, and **DHADC**-CN^- species were calculated and expressed as fluorescein-**DHADC**, fluorescein-**DHADC**-Zn^{2+}, and fluorescein-**DHADC**-CN^-. The quantum yields were calculated with the following equation [44].

$$\Phi_{F,S} = \Phi_{F,R} \frac{A_R F_S}{A_S F_R} \left(\frac{n_S}{n_R}\right)^2$$

Φ_F is quantum yield, A is absorbance, F is the area of fluorescence emission curve, n is refractive index of the solvent, S is test sample, and R is a reference sample.

2.9. Quantification of Zn^{2+} in Real Samples

For fluorescent analysis in real samples, drinking water and tap water were obtained from our laboratory. The fluorescent analysis was carried out by adding 3.0 μL (10^{-2} M) of compound **DHADC** and 0.30 mL of a bis-tris buffer (10^{-2} M) to a 2.697 mL real sample solution having Zn^{2+}. Solutions were thoroughly blended and remained at 20 °C for 5 min. Their fluorescence spectra were obtained.

2.10. Imaging in Live Cells and Zebrafish

In media containing 100 mg/mL streptomycin, the Eagle Medium, 10.0% fetal bovine serum, and 100 U/mL penicillin HeLa cells were kept. The cells grew in a humidified condition at 37.0 °C under 5% CO_2. They were then put onto a 12 well plate (SPL Life Sciences, Pocheon, Gyeonggi-do, Republic of Korea) at a density of 1×10^4 cells/0.1 mL, cells were seeded and then incubated at 37.0 °C for 20 h. For fluorescent imaging tests, cells were treated with compound **DHADC** (dissolved in DMSO, 3 $\times 10^{-2}$ mM) for 10 min, followed by the incubation of $Zn(NO_3)_2$ (dissolved in water, 5.0 mM) for 10 min. A EVOS FL fluorescent microscope was employed for imaging [emission 510 (±21) nm; excitation 470 (±11) nm].

The wild types of zebrafish (AB line) were incubated at 29 °C on a 14 h light/12 h dark cycle in E2 media (1×10^{-3} M $MgSO_4$, 1×10^{-3} M $CaCl_2$, 1.5×10^{-4} M KH_2PO_4, 1.5×10^{-2} M NaCl, 5×10^{-5} M Na_2HPO_4, 1×10^{-4} M KCl, 0.5 mg/L MB (methylene blue), and 0.7 mM $NaHCO_3$ at pH 7.2). Six-day-old zebrafish were prepared for fluorescence bio-imaging in vivo. Zebrafish were fed with only 5×10^{-3} mM of **DHADC** in E2 media having 0.05% DMSO at 29 °C for 10 min. After the zebrafish were rinsed with E2 media to get rid of the remaining **DHADC**, the zebrafish were fed with the solution and had a wide range of concentrations of Zn^{2+} (20, 50, 100, and 200 μM) for 10 min at 29 °C. They were rinsed with E2 media again and then 0.01% ethyl-3-aminobenzoate methanesulfonate was added for the fixed orientation of zebrafish. A fluorescent microscope (MDG36, Leica) was employed to image all zebrafish (λ_{ex} = 450–490 nm. λ_{em} = 500–550 nm). By using Icy software, the mean fluorescence intensity was determined.

3. Results and Discussion

Probe **DHADC** was provided by the reaction of 4-diethylaminosalicylaldehyde and 3-aminothiophene-2-carboxamide in ethanol (72% yield, Scheme 1), and affirmed by ^{13}C and ^{1}H NMR and ESI-mass instrument.

*3.1. Fluorescence Investigation of **DHADC** to Metal Cations*

The sensing selectivity of **DHADC** was examined in the presence of various cations (Ni^{2+}, Mn^{2+}, Ga^{3+}, Fe^{3+}, Na^{+}, In^{2+}, Zn^{2+}, Ca^{2+}, Cd^{2+}, Cu^{2+}, Pb^{2+}, Mg^{2+}, Cr^{3+}, Co^{2+}, K^{+}, Al^{3+}, and Fe^{2+}) in bis-tris buffer (Figure 1). By adding each metal ion (140 equiv), Zn^{2+} only exhibited a striking fluorescence increase (ca. 4500%) (λ_{ex} = 446 nm, λ_{em} = 508 nm). Instead, other cations did not increase the fluorescence. These outcomes illustrated that compound **DHADC** showed high discrimination towards Zn^{2+}.

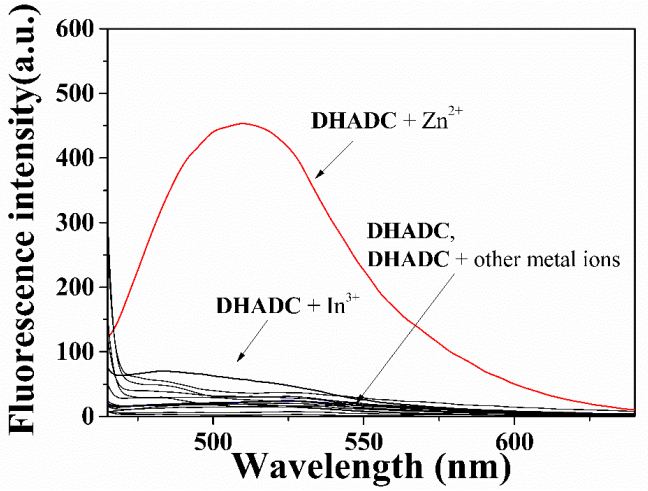

Figure 1. Fluorescent changes of **DHADC** (1×10^{-5} M) with various cations (Al^{3+}, Ga^{3+}, In^{3+}, Cd^{2+}, Cu^{2+}, Fe^{2+}, Fe^{3+}, Mg^{2+}, Cr^{3+}, Hg^{2+}, Ag^{+}, Co^{2+}, Ni^{2+}, Na^{+}, K^{+}, Mn^{2+}, and Pb^{2+},140 equiv; λ_{ex} = 446 nm; slit width = 10 nm).

To examine the interaction between **DHADC** and Zn^{2+}, fluorescent titration of compound **DHADC** to zinc ion was executed (Figure 2). The emission (508 nm) of compound **DHADC** steadily increased and indicated a maximum at 140 equiv. (λ_{ex} = 446 nm). Quantum yields (Φ) of 0.0003 (±0.0001) and 0.0135 (±0.0004) were determined for **DHADC** and **DHADC**-Zn^{2+} (Figure S1; λ_{ex} = 464 nm). Binding type of **DHADC** with zinc ion was also analyzed by UV-visible titration (Figure S2). By adding Zn^{2+} to compound **DHADC**, the peaks of 320 and 470 nm increased continuously, and that of 430 nm decreased. There were two definite isosbestic points (380 and 447 nm), meaning that the binding of **DHADC** to Zn^{2+} formed one product.

The binding process of **DHADC** and zinc ion was proposed to be a 1:1 interaction with the analysis of Job plot (Figure S3; λ_{ex} = 446 nm, λ_{em} = 508 nm) [45]. The 1:1 interaction of **DHADC**-Zn^{2+} was affirmed by the ESI-mass search (Figure S4). The mass data displayed that the peak of 458.00 (*m*/*z*) was reminiscent of [**DHADC**(-H^{+}) + Zn^{2+} + DMSO]$^{+}$ (calculated at 458.05). With fluorescent titration, the association constant (*K*) for **DHADC** with Zn^{2+} was given as 1.6×10^{3} (±31) M^{-1} by the equation of Benesi–Hildebrand (Figure S5) [46]. The constant was in the range of those (K = 1–10^{12}) of previously announced probes for Zn^{2+} [47–49]. The binding process of compound **DHADC** with Zn^{2+} was further inspected by the titration of ^{1}H NMR (Figure 3). With addition of Zn^{2+} (1 equiv.), the imine proton of 8.76 ppm was moved to downfield. At the same time, the protons of the thiophene moiety and the benzene ring were also moved to downfield. These results demonstrated that the N atom in the imine component and the O atom in the amide component may bind to Zn^{2+}. No shift of the proton signals was monitored with the addition of more Zn^{2+} ions, which was indicative of

a 1:1 binding of **DHADC**-Zn^{2+} species (Scheme 2). On the basis of the previous studies [34,50], the fluorescence turn-on mechanism of **DHADC** for Zn^{2+} might have the CHEF effect (chelation-enhanced fluorescence). During complexation of **DHADC** and Zn^{2+}, the non-radiative transitions such as rotation and vibration were inhibited and the radiative transition was enhanced.

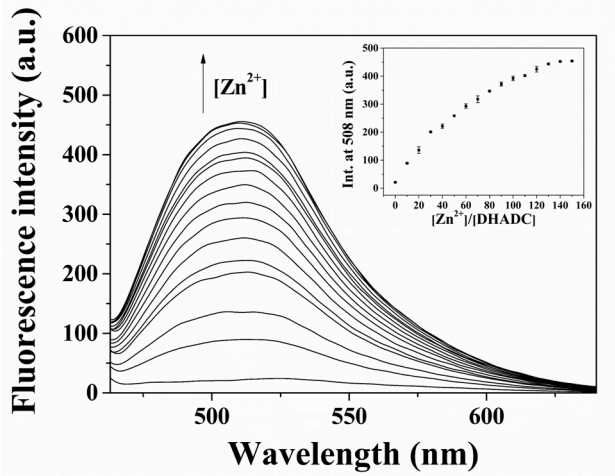

Figure 2. Fluorescent changes of **DHADC** (1×10^{-5} M) with different amounts of Zn^{2+} (from 0 to 150 equiv.). λ_{ex} = 446 nm; slit width = 10 nm. Inset: Fluorescence intensity at 508 nm vs. the amounts of Zn^{2+}.

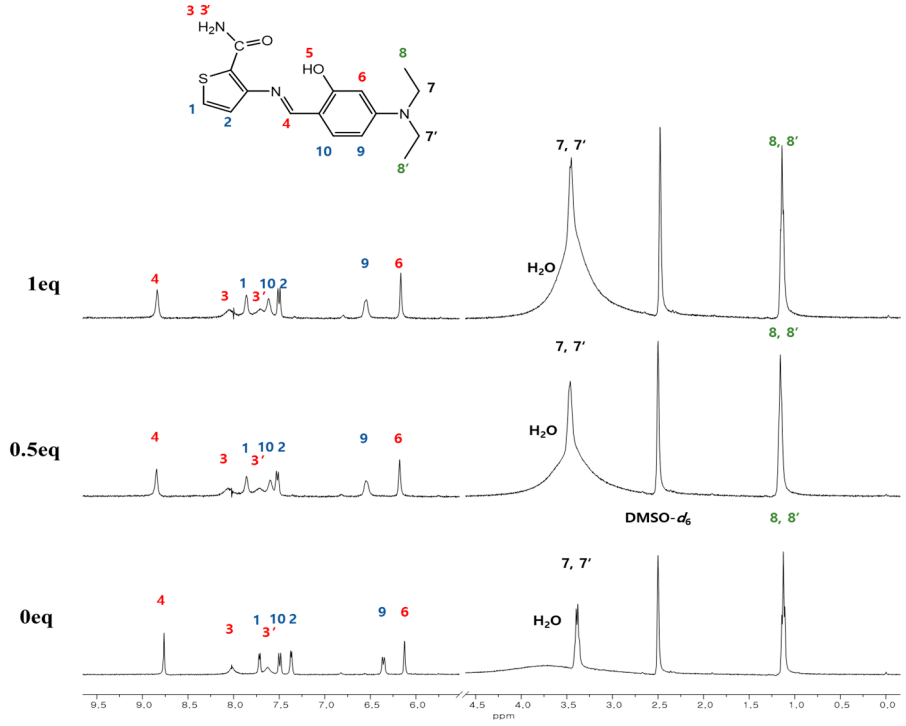

Figure 3. ^{1}H NMR titration of **DHADC** upon addition of Zn^{2+} (0, 0.5, and 1 equiv.).

To test the practicable capability of compound **DHADC** as a Zn^{2+} detector, the competitive study was executed in a mixture of Zn^{2+} (140 equiv.) and various interfering ions (140 equiv.; Al^{3+}, Pb^{2+}, Ga^{3+}, Fe^{3+}, K^+, In^{2+}, Ni^{2+}, Cd^{2+}, Mg^{2+}, Fe^{2+}, Cr^{3+}, Na^+, Ca^{2+}, Mn^{2+}, Co^{2+}, and Cu^{2+}) (Figure S6; λ_{ex} = 446 nm, λ_{em} = 508 nm). Cu^{2+} fully interfered, and Fe^{3+}, Cr^{3+}, Fe^{2+}, Co^{2+}, and In^{3+} quenched 89%, 83%, 67%, 65%, and 22% of the fluorescence obtained with zinc ion alone. Therefore, the paramagnetic metal ions might be avoided for the applicability of the sensor in biological matrices. For practicable

applications, the pH response of **DHADC**-Zn^{2+} was investigated at a wide variety of pH (2–12) (Figure S7; λ_{ex} = 446 nm, λ_{em} = 508 nm). **DHADC**-Zn^{2+} species exhibited a momentous fluorescence enhancement between pH 7 and 10. Therefore, Zn^{2+} could obviously be sensed by the fluorescent analysis with compound **DHADC** over the physiologically and environmentally important pH scope of 7.0–8.4 [51].

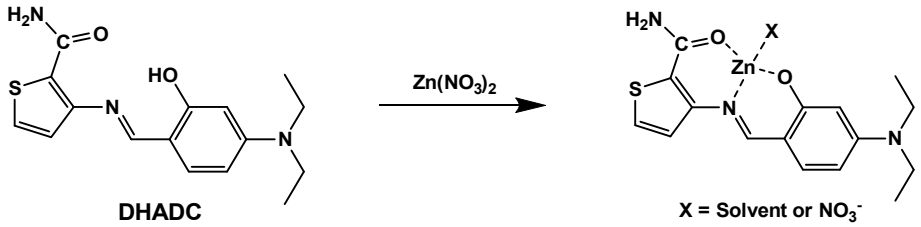

Scheme 2. Proposed structure of **DHADC**-Zn^{2+}.

We established a calibration plot for the quantitative measurement of Zn^{2+} by compound **DHADC** (λ_{ex} = 446 nm, λ_{em} = 508 nm). Compound **DHADC** exhibited a satisfactory linearity between its intensity and the concentration of Zn^{2+}, indicating that compound **DHADC** could be a possible choice for the quantitative measurement of Zn^{2+}. With the use of 3 σ/slope [52], the detection limit was determined by 2.55 (±0.05) μM (Figure 4), which was much lower than the guideline (76 μM) recommended by the World Health Organization (WHO) [53,54]. To confirm the practicable ability of compound **DHADC** to Zn^{2+} in environmental samples, the samples of tap and drinking water were chosen (Table 1; λ_{ex} = 446 nm, λ_{em} = 508 nm). Acceptable recoveries and relative standard deviation (R.S.D.) values were obtained for the samples. Thus, compound **DHADC** can be operational for the measurement of Zn^{2+} in practical applications.

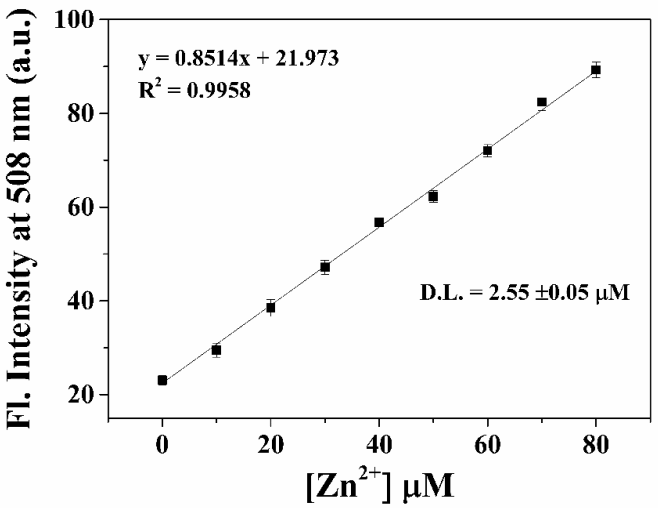

Figure 4. Fluorescence intensities (at 508 nm) of **DHADC** as a function of Zn(II) concentration ([**DHADC**] = 10 μmol/L and [Zn(II)] = 10–80 μmol/L). Conditions: All samples were conducted in bis-tris buffer solution (10 mM bis-tris, pH 7.0). λ_{ex} = 446 nm; and slit width = 10 nm.

In order to assess the sensing feasibility for biological applications of **DHADC**, we conducted fluorescent imaging experiments for sensing Zn^{2+} in living cells (Figure 5). We first incubated the HeLa cells with **DHADC** (30 μM) for 20 min. Then, the fluorescent emission in cells was not discovered without Zn^{2+}. In contrast, the cells cultured with Zn^{2+} showed significantly increased fluorescence intensity. To further demonstrate the ability of **DHADC** in living organisms, the experiment for fluorescence imaging was carried out with zebrafish (Figure 6). When the zebrafish was incubated with **DHADC** (5 μM, a), there was no fluorescence signal. However, with increasing concentrations

(20–200 μM, b–e) of Zn^{2+}, the fluorescence signal gradually increased. By using Icy software, the mean fluorescent emission of the images was analyzed (Figure S8). The limit of detection was analyzed to be 21.44 (±2.6) μM. Thus, compound **DHADC** may be applied to intracellular sensing of Zn^{2+} in living organisms.

Table 1. Determination of zinc ion concentration [1].

Sample	Zn(II) Added (μmol/L)	Zn(II) Found (μmol/L)	Recovery (%)	R.S.D. (n = 3) (%)
Drinking Water	0	0	-	-
	20	19.1 ± 0.6	95.5 ± 1.0	3.96 ± 0.5
Tap Water	0	0	-	-
	20	19.7 ± 1.0	98.5 ± 1.4	1.51 ± 1.1

[1] Conditions: [**DHADC**] = 10 μM in 10 mM bis-tris buffer (pH 7.0).

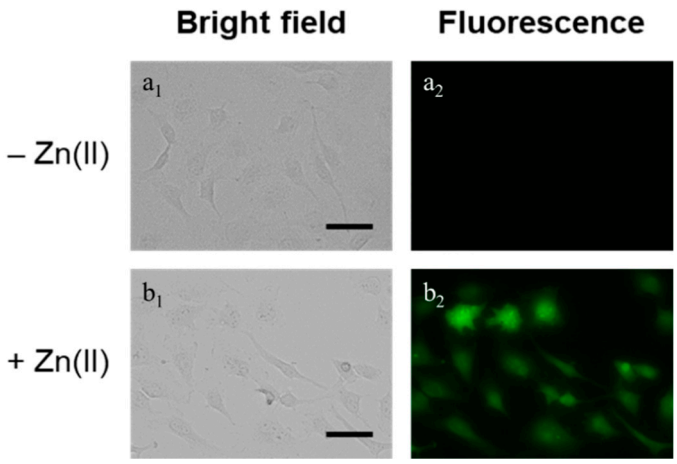

Figure 5. Fluorescent imaging of HeLa cells incubated with **DHADC** and Zn(II). Cells were incubated with **DHADC** and Zn(II) for 20 min. (**a_1**,**a_2**): **DHADC** only; (**b_1**,**b_2**): **DHADC** with zinc ion. Conditions: [**DHADC**] = 30 μM; [Zn(II)] = 5 mM; 37 °C; and 5% CO_2. λ_{ex} = 470 ± 11 nm. λ_{em} = 510 nm. Scale bar was 50 μm.

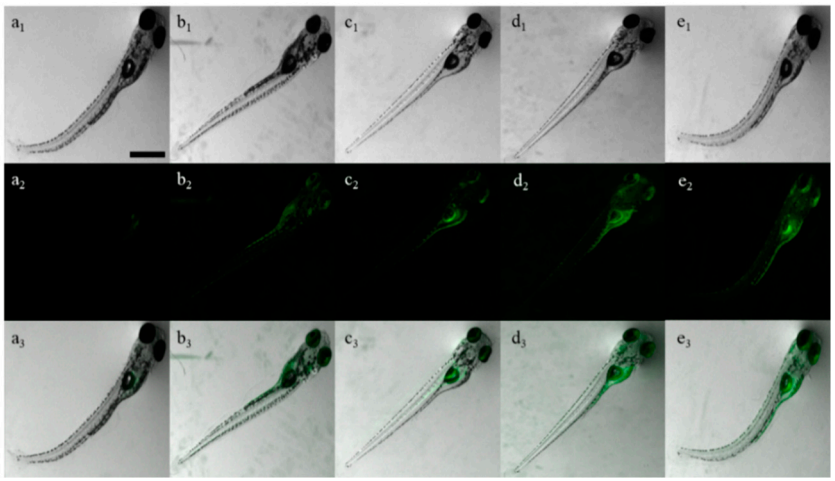

Figure 6. Fluorescence images of zebrafish (6-day-old) incubated with **DHADC** followed by addition of zinc ion. Top line: bright-field image; middle line: fluorescent image; and bottom line: overlay image. (**a_1**–**a_3**): **DHADC** only; (**b_1**–**b_3**): **DHADC** with 20 μM zinc ion; (**c_1**–**c_3**): **DHADC** with 50 μM zinc ion; (**d_1**–**d_3**): **DHADC** with 100 μM zinc ion; and (**e_1**–**e_3**): **DHADC** with 200 μM zinc ion. [**DHADC**] = 5 μM. λ_{ex} = 450–490 nm. λ_{em} = 500–550 nm. Scale bar: 1 mm.

3.2. Fluorescence Studies of Compound ***DHADC*** to CN^-

The fluorescence sensing capability of **DHADC** to a variety of anions in bis-tris buffer/acetonitrile solution (5:95) was examined (Figure 7; λ_{ex} = 459 nm, λ_{em} = 528 nm). The fluorescent spectra of **DHADC** with diverse types of anions (I^-, S^{2-}, $H_2PO_4^-$, Cl^-, N_3^-, F^-, BzO^-, Br^-, OAc^-, SCN^-, and NO_2^-) showed very weak intensities. In contrast, there was a significant enhancement of fluorescence at 528 nm by adding 100 equiv. of CN^-. These outcomes indicated that compound **DHADC** could have a potential function as a choosy fluorescence receptor for CN^-.

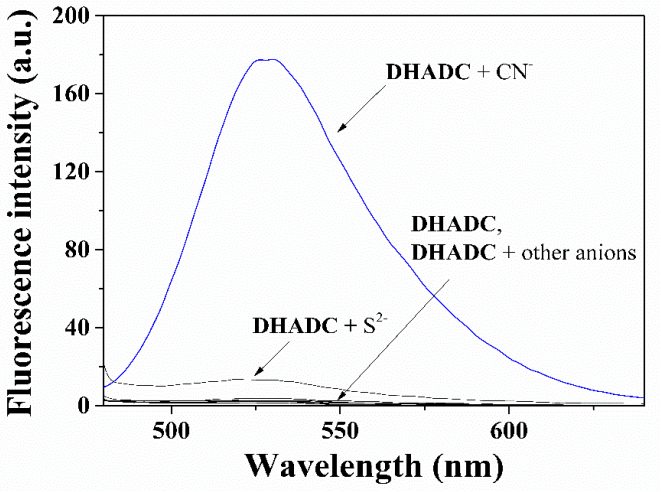

Figure 7. Fluorescent changes of **DHADC** (1×10^{-5} M) with other anions (OAc^-, F^-, Cl^-, Br^-, I^-, $H_2PO_4^-$, BzO^-, N_3^-, SCN^-, NO_2^-, and S^{2-}, 100 equiv.; λ_{ex} = 459 nm; slit width = 10 nm).

To examine the influence of increasing levels of CN^- to **DHADC** solution, the fluorescence titration was carried out (Figure 8; λ_{ex} = 459 nm, λ_{em} = 528 nm). When the CN^- (0–120 equiv.) was added into **DHADC** solution, the fluorescence emission continuously increased at 528 nm and showed a maximum with 100 equiv. Quantum yields (Φ) of 0.0063 (±0.0004) and 0.1118 (±0.0003) were analyzed for **DHADC** and **DHADC**-CN^- (Figure S1). The binding character of compound **DHADC** with CN^- was inspected by UV-visible titration test (Figure S9). With the addition of cyanide to compound **DHADC**, the peaks at 315 and 475 nm increased consistently, and 390 nm decreased continuously with two definite isosbestic points (345 and 425 nm).

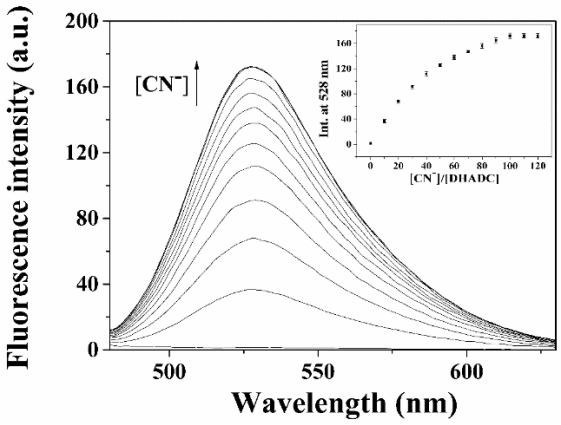

Figure 8. Fluorescent changes of **DHADC** (1×10^{-5} M) with different amounts of cyanide (from 0 to 120 equiv.). λ_{ex} = 459 nm; slit width = 10 nm. Inset: Fluorescence intensity at 528 nm vs. the amounts of cyanide.

To investigate the binding mode of **DHADC** and CN^-, Job plot analysis was performed (Figure S10; λ_{ex} = 459 nm, λ_{em} = 528 nm) [45]. This result showed a 1:1 complexation, which was affirmed by ESI-MS analysis (Figure S11). Addition of CN^- (1 equiv.) into compound **DHADC** exhibited the production of the [**DHADC** - H^+]$^-$ [*m/z:* 316.21; calculated at 316.11]. With the results of the fluorescent titration, the *K* value for **DHADC** with CN^- was given as 1.6 × 10^3 (±50) M^{-1} (Figure S12). The detection limit (3σ/slope) was determined by 44.6 (±1.5) μM (Figure 9) [52].

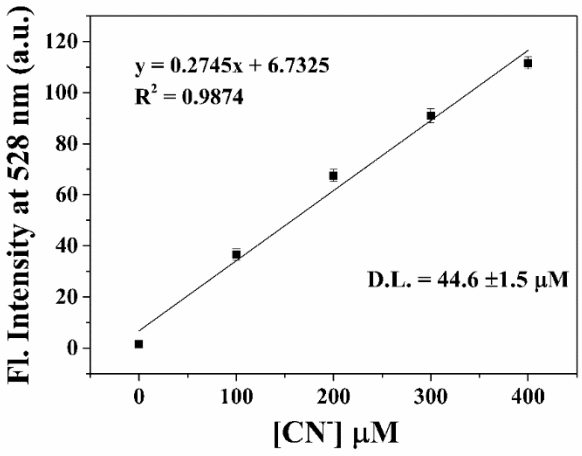

Figure 9. Determination of the detection limit of **DHADC** (10 μM) for CN^- based on the change of intensity at 528 nm. λ_{ex} = 459 nm; slit width = 10 nm.

To elucidate the detection process of compound **DHADC** with CN^-, we carried out the titration experiments of ^{1}H NMR (Figure S13). The proton of the hydroxyl component did not show up because of the possible inter or intra-molecular hydrogen bonds [55]. With the addition of CN (2 equiv.) to compound **DHADC**, all protons of the thiophene group and the benzene ring shifted to upfield. In contrast, one of the amide protons (H_3) was shifted to downfield, suggesting that the H_3 proton might hydrogen bond to CN^- or HCN species (Scheme 3). These outcomes implied that the negative charge generated from the deprotonation of compound **DHADC** by cyanide was delocalized through the **DHADC** [56]. No movement of the proton signals was detected with addition of more amounts of CN^- (>2 equiv.). On the basis of the previous studies and our experimental data [34,57,58], we can propose that the deprotonation of **DHADC** could cause the suppression of ICT (intramolecular charge transfer), which induces fluorescence turn-on of **DHADC**-H^+ species. With the analysis results of ESI-mass, ^{1}H NMR study and Job plot, the possible recognizing process of compound **DHADC** with CN^- was depicted in Scheme 3.

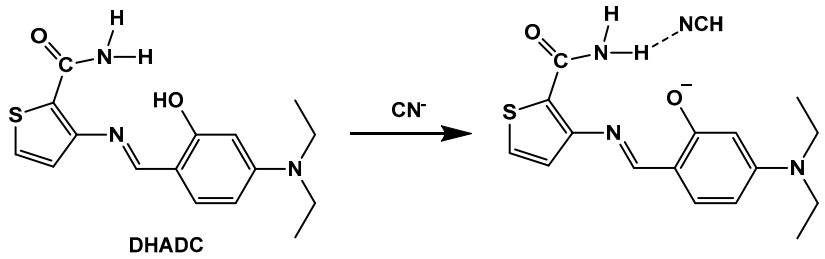

Scheme 3. Proposed sensing mechanism of **DHADC** for CN^-.

To inspect the inhibition of different types of anions, the competitive tests were achieved and are shown in Figure 10 (λ_{ex} = 459 nm, λ_{em} = 528 nm). Compound **DHADC** was mixed with CN^- (100 equiv.) and a wide variety of anions (S^{2-}, F^-, BzO^-, Cl^-, SCN^-, Br^-, NO_2^-, OAc^-, N_3^-, $H_2PO_4^-$, and I^-; 100 equiv.). Some inhibition was observed with F^-, but its fluorescence was still discernible.

These observations illustrated that compound **DHADC** may be an excellent selective fluorescence detector for CN^-.

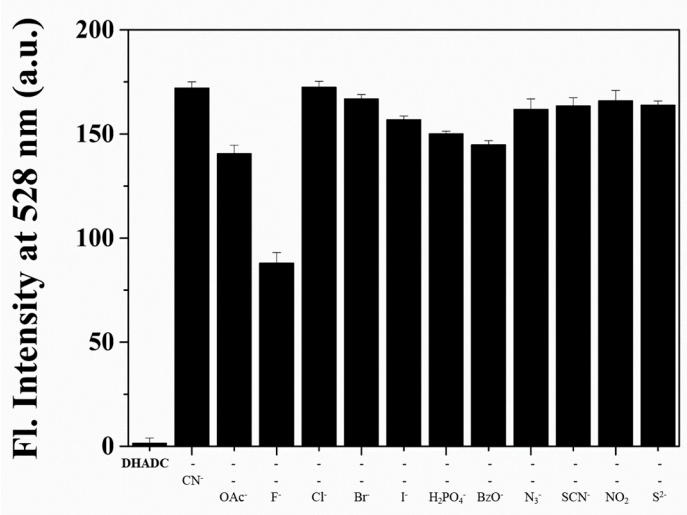

Figure 10. Competitive test of **DHADC** (1×10^{-5} M) to cyanide (100 equiv.) with other anions (100 equiv.). λ_{ex} = 459 nm; slit width = 10 nm.

4. Conclusions

We demonstrated a unique fluorescent turn-on probe **DHADC** having a thiophene moiety. Compound **DHADC** could selectively sense Zn^{2+} and CN^- through fluorescence enhancement. Binding ratios of compound **DHADC** with Zn^{2+} and CN^- were proposed to be 1:1, with the analysis of ESI-mass data and Job plots. Detection limits for zinc ion and CN^- were 2.55 (±0.05) μM and 44.6 (±1.5) μM, respectively. The value for zinc ion was far below the standard (76 μM) of the WHO. Importantly, compound **DHADC** could be used to analyze zinc ion in water samples and to image zinc ion in both zebrafish and live cells. Additionally, compound **DHADC** could detect CN^- with little interference of competitive anions. Moreover, the detection processes of **DHADC** with Zn^{2+} and CN^- were proposed through ^{1}H NMR titrations and ESI-Mass analyses. Therefore, the results observed in this study illustrate that **DHADC** can be a detector to selectively detect Zn^{2+} and CN^- by the fluorescent turn-on method in aqueous and living organisms.

Supplementary Materials: The following are available online at http://www.mdpi.com/1424-8220/19/24/5458/s1, Table S1: Examples of chemosensors for detecting both Zn^{2+} and CN^-, Figure S1: (a) Fluorescent (λ_{ex} = 464 nm) and (b) absorption spectra of **DHADC** (3 μM), **DHADC**+Zn^{2+} (140 equiv.) and fluorescein. (c) Fluorescent (λ_{ex} = 459 nm) and (d) absorption spectra of **DHADC** (10 μM), **DHADC**+CN^- (100 equiv.) and fluorescein; slit width = 10 nm, Figure S2: UV-vis absorption spectra of **DHADC** (10 μM) obtained during the titration with $Zn(NO_3)_2$ (0–140 equiv.), Figure S3: (a) Fluorescence spectra of Job plot for the binding of **DHADC** with Zn^{2+}. (b) Intensity at 508 nm was plotted as a function of the molar ratio $[Zn^{2+}]/([\mathbf{DHADC}] + [Zn^{2+}])$. The total concentration of zinc ion with **DHADC** was 7.0×10^{-5} M. λ_{ex} = 446 nm; slit width = 10 nm, Figure S4: Positive-ion electrospray ionization mass spectrum of **DHADC** (100 μM) upon addition of 1 equiv. of Zn^{2+}, Figure S5: Benesi-Hildebrand equation plot (intensity at 508 nm) of **DHADC**, assuming 1:1 stoichiometry for association between **DHADC** and Zn^{2+}. λ_{ex} = 446 nm; slit width = 10 nm, Figure S6: Competitive selectivity of **DHADC** (10 μM) toward Zn^{2+} (140 equiv.) in the presence of other metal ions (140 equiv.). λ_{ex} = 446 nm; slit width = 10 nm, Figure S7: Fluorescence intensities (at 508 nm) of **DHADC** and **DHADC**-Zn^{2+} complex, respectively, at different pH values (2–12). λ_{ex} = 446 nm; slit width = 10 nm, Figure S8: Quantification of mean fluorescence intensity in Fig. 6 (a_2, b_2, c_2, d_2 and e_2), Figure S9: UV-vis absorption spectra of **DHADC** (10 μM) obtained during the titration with CN^- (0–100 equiv.), Figure S10: Job plot for the binding of **DHADC** with CN^-. Absorbance at 440 nm was plotted as a function of the molar ratio $[CN^-]/([\mathbf{DHADC}] + [CN^-])$. The total concentration of CN^- with **DHADC** was 2.0×10^{-4} M, Figure S11: Negative-ion electrospray ionization mass spectrum of **DHADC** (100 μM) upon addition of 1 equiv. of CN^-, Figure S12: Benesi-Hildebrand equation plot (intensity at 528 nm) of **DHADC**, assuming 1:1 stoichiometry for association between **DHADC** and CN^-. λ_{ex} = 459 nm; slit width = 10 nm, Figure S13: ^{1}H NMR titration of **DHADC** with CN^-.

Author Contributions: M.S.K. and C.K. provided the initial idea for this work; D.Y., J.B.C., H.S., H.L. and M.K. contributed to the collection and analysis of field test data; K.-T.K. and M.H.L. contributed to the analyses of results; M.S.K. and C.K. wrote the paper.

Funding: KEITI (Korea Environment Industry & Technology Institute) (2016001970001) and NRF (National Research Foundation of Korea) (2018R1A2B6001686) are thankfully acknowledged.

Conflicts of Interest: The authors declare no conflicts of interest.

References

1. Aragay, G.; Pons, J.; Merkoçi, A. Recent trends in macro-, micro-, and nanomaterial-based tools and strategies for heavy-metal detection. *Chem. Rev.* **2011**, *111*, 3433–3458. [CrossRef] [PubMed]
2. Chen, Y.; Bai, Y.; Han, Z.; He, W.; Guo, Z. Photoluminescence imaging of Zn^{2+} in living systems. *Chem. Soc. Rev.* **2015**, *44*, 4517–4546. [CrossRef] [PubMed]
3. Xu, Z.; Yoon, J.; Spring, D.R. Fluorescent chemosensors for Zn^{2+}. *Chem. Soc. Rev.* **2010**, *39*, 1996–2006. [CrossRef] [PubMed]
4. Li, W.; Tian, X.; Huang, B.; Li, H.; Zhao, X.; Gao, S.; Zheng, J.; Zhang, X.; Zhou, H.; Tian, Y.; et al. Triphenylamine-based Schiff bases as the High sensitive Al^{3+} or Zn^{2+} fluorescence turn-on probe: Mechanism and application in vitro and in vivo. *Biosens. Bioelectron.* **2016**, *77*, 530–536. [CrossRef]
5. Choi, J.Y.; Kim, D.; Yoon, J. A highly selective "turn-on" fluorescent chemosensor based on hydroxy pyrene-hydrazone derivative for Zn^{2+}. *Dyes Pigm.* **2013**, *96*, 176–179. [CrossRef]
6. Hagimori, M.; Taniura, M.; Mizuyama, N.; Karimine, Y.; Kawakami, S.; Saji, H.; Mukai, T. Synthesis of a novel pyrazine-pyridone biheteroaryl-based fluorescence sensor and detection of endogenous labile zinc ions in lung cancer cells. *Sensors* **2019**, *19*, 2049. [CrossRef]
7. Guo, Z.; Kim, G.H.; Yoon, J.; Shin, I. Synthesis of a highly Zn^{2+}-selective cyanine-based probe and its use for tracing endogenous zinc ions in cells and organisms. *Nat. Protoc.* **2014**, *9*, 1245–1254. [CrossRef]
8. Sohrabi, M.; Amirnasr, M.; Farrokhpour, H.; Meghdadi, S. A single chemosensor with combined ionophore/fluorophore moieties acting as a fluorescent "Off-On" Zn^{2+} sensor and a colorimetric sensor for Cu^{2+}: Experimental, logic gate behavior and TD-DFT calculations. *Sens. Actuators B Chem.* **2017**, *250*, 647–658. [CrossRef]
9. Bhanja, A.K.; Patra, C.; Mondal, S.; Mishra, S.; Saha, K.D.; Sinha, C. Macrocycle aza-crown chromogenic reagent to Al^{3+} and fluorescence sensor for Zn^{2+} and Al^{3+} along with live cell application and logic operation. *Sens. Actuators B Chem.* **2017**, *252*, 257–267. [CrossRef]
10. Kim, M.S.; Jo, T.G.; Ahn, H.M.; Kim, C. A Colorimetric and Fluorescent Chemosensor for the Selective Detection of Cu^{2+} and Zn^{2+} Ions. *J. Fluoresc.* **2016**, *27*, 357–367. [CrossRef]
11. Das, B.; Jana, A.; Mahapatra, A.D.; Chattopadhyay, D.; Dhara, A.; Mabhai, S.; Dey, S. Fluorescein derived Schiff base as fluorimetric zinc(II) sensor via 'turn on' response and its application in live cell imaging. *Spectrochim. Acta A* **2019**, *212*, 222–231. [CrossRef] [PubMed]
12. Yang, X.; Li, Y.; Ding, Y.; Zhao, Z.; Zhang, Y.; Liu, X.; Fu, Z.; Cui, Y.; Sun, G.; Zhang, G.; et al. Ratiometric & reversible fluorescent sensing of NaCN by an effective probe based on phenanthro [9,10-d]imidazole platform. *Sens. Actuators B Chem.* **2017**, *253*, 478–487.
13. Maurya, N.; Bhardwaj, S.; Singh, A.K. A modest colorimetric chemosensor for investigation of CN^- in semi-aqueous environment with high selectivity and sensitivity. *Sens. Actuators B Chem.* **2016**, *229*, 483–491. [CrossRef]
14. Sarkar, A.; Bhattacharyya, S.; Mukherjee, A. Colorimetric detection of fluoride ions by anthraimidazoledione based sensors in the presence of Cu(II) ions. *Dalton Trans.* **2016**, *45*, 1166–1175. [CrossRef]
15. Jo, T.G.; Na, Y.J.; Lee, J.J.; Lee, M.M.; Lee, S.Y.; Kim, C. A multifunctional colorimetric chemosensor for cyanide and copper(II) ions. *Sens. Actuators B Chem.* **2015**, *211*, 498–506. [CrossRef]
16. You, G.R.; Park, G.J.; Lee, J.J.; Kim, C. A colorimetric sensor for the sequential detection of Cu^{2+} and CN^- in fully aqueous media: Practical performance of Cu^{2+}. *Dalton Trans.* **2015**, *44*, 9120–9129. [CrossRef]
17. Sheshashena Reddy, T.; Maragani, R.; Misra, R. Triarylborane substituted naphthalimide as a fluoride and cyanide ion sensor. *Dalton Trans.* **2016**, *45*, 2549–2553. [CrossRef]

18. Kim, D.; Na, S.Y.; Kim, H.J. A fluorescence turn-on probe for a catalytic amount of cyanides through the cyanide-mediated cinnamate-to-coumarin transformation. *Sens. Actuators B Chem.* **2016**, *226*, 227–231. [CrossRef]
19. Hachiya, H.; Ito, S.; Fushinuki, Y.; Masadome, T.; Asano, Y.; Imato, T. Continuous monitoring for cyanide in waste water with a galvanic hydrogen cyanide sensor using a purge system. *Talanta* **1999**, *48*, 997–1004. [CrossRef]
20. Zhang, X.; Chen, S.; Jin, S.; Lu, X.; Li, L.; Chen, X.; Shu, Q. Naphthalene based lab-on-a-molecule for the highly selective and sensitive detection of CN^- and Ag^+ in aqueous solution. *Sens. Actuators B Chem.* **2016**, *237*, 367–372. [CrossRef]
21. Elsafy, A.G.; Al-Easa, H.S.; Hijji, Y.M. Substituted 2-aminobenzothiazoles salicylidenes synthesis and characterization as cyanide sensors in aqueous medium. *Sensors* **2018**, *18*, 2219. [CrossRef] [PubMed]
22. Khairnar, N.; Tayade, K.; Sahoo, S.K.; Bondhopadhyay, B.; Basu, A.; Singh, J.; Singh, N.; Gite, V.; Kuwar, A. A highly selective fluorescent 'turn-on' chemosensor for Zn^{2+} based on a benzothiazole conjugate: Their applicability in live cell imaging and use of the resultant complex as a secondary sensor of CN^-. *Dalton Trans.* **2015**, *44*, 2097–2102. [CrossRef] [PubMed]
23. "First pass phenomenon" of inhaled gas in the fire victims. *Forensic Sci. Int.* **1990**, *46*, 203–208. [CrossRef]
24. Shi, Z.; Tu, Y.; Wang, R.; Liu, G.; Pu, S. Highly sensitive and selective turn-on fluorescent sensor for dual recognition of Cu^{2+} and CN^- based on a methylquinoline derivative. *Dyes Pigm.* **2018**, *149*, 764–773. [CrossRef]
25. Ryu, K.Y.; Lee, J.J.; Kim, J.A.; Park, D.Y.; Kim, C. Colorimetric chemosensor for multiple targets, Cu^{2+}, CN^- and S^{2-}. *RSC Adv.* **2016**, *6*, 16586–16597. [CrossRef]
26. Liang, M.; Wang, K.; Guan, R.; Liu, Z.; Cao, D.; Wu, Q.; Shan, Y.; Xu, Y.; Luo, Z.; Yin, K.; et al. Several hemicyanine dyes as fluorescence chemosensors for cyanide anions. *Spectrochim. Acta A* **2016**, *169*, 34–38. [CrossRef]
27. Keshav, K.; Torawane, P.; Kumar Kumawat, M.; Tayade, K.; Sahoo, S.K.; Srivastava, R.; Kuwar, A. Highly selective optical and reversible dual-path chemosensor for cyanide detection and its application in live cells imaging. *Biosens. Bioelectron.* **2017**, *92*, 95–100. [CrossRef]
28. Zhang, W.; Xu, K.; Yue, L.; Shao, Z.; Feng, Y.; Fang, M. Two-dimensional carbazole-based derivatives as versatile chemosensors for colorimetric detection of cyanide and two-photon fluorescence imaging of viscosity in vitro. *Dyes Pigm.* **2017**, *137*, 560–568. [CrossRef]
29. Park, G.J.; Hwang, I.H.; Song, E.J.; Kim, H.; Kim, C. A colorimetric and fluorescent sensor for sequential detection of copper ion and cyanide. *Tetrahedron* **2014**, *70*, 2822–2828. [CrossRef]
30. Liu, D.; Yin, X.; Deng, X.; Shi, J.; Zhu, H.; Shang, Z.; Chen, J.; Yang, G.; He, H. 1, 8-Naphthalimide-based fluorescent sensor with highly selective and sensitive detection of Zn^{2+} in aqueous solution and living cells. *Inorg. Chem. Commun.* **2019**, *106*, 43–47. [CrossRef]
31. Peng, M.J.; Guo, Y.; Yang, X.F.; Suzenet, F.; Li, J.; Li, C.W.; Duan, Y.W. Coumarin-hemicyanine conjugates as novel reaction-based sensors for cyanide detection: Convenient synthesis and ICT mechanism. *RSC Adv.* **2014**, *4*, 19077–19085. [CrossRef]
32. Suganya, S.; Ravindran, E.; Mahato, M.K.; Prasad, E. Orange emitting fluorescence probe for the selective detection of cyanide ion in solution and solid states. *Sens. Actuators B* **2019**, *291*, 426–432. [CrossRef]
33. Rezaeian, K.; Khanmohammadi, H.; Gholizadeh Dogaheh, S. Studies on a multifunctional chromo-fluorogenic sensor for dual channel recognition of Zn^{2+} and CN^- ions in aqueous media: Mimicking multiple molecular logic gates and memory devices. *New J. Chem.* **2018**, *42*, 2158–2166. [CrossRef]
34. Gao, W.; Li, H.; Zhang, Y.; Pu, S. A highly selective diarylethene chemosensor for dual channel recognition of CN^- and Zn^{2+} and its application. *Tetrahedron* **2019**, *75*, 2538–2546. [CrossRef]
35. Hu, J.H.; Sun, Y.; Qi, J.; Li, Q.; Wei, T.B. A new unsymmetrical azine derivative based on coumarin group as dual-modal sensor for CN^- and fluorescent "OFF–ON" for Zn^{2+}. *Spectrochim. Acta A* **2017**, *175*, 125–133. [CrossRef]
36. Sun, S.; Shu, Q.; Lin, P.; Li, Y.; Jin, S.; Chen, X.; Wang, D. Triphenylamine based lab-on-a-molecule for the highly selective and sensitive detection of Zn^{2+} and CN^- in aqueous solution. *RSC Adv.* **2016**, *6*, 93826–93831. [CrossRef]

37. Li, Y.; Gu, Z.; He, T.; Yuan, X.; Zhang, Y.; Xu, Z.; Qiu, H.; Zhang, Q.; Yin, S. Terpyridyl-based triphenylamine derivatives with aggregation-induced emission characteristics for selective detection of Zn^{2+}, Cd^{2+} and CN^{-} ions and application in cell imaging. *Dyes Pigm.* **2020**, *173*, 107969. [CrossRef]
38. Anand, T.; Kumar SK, A.; Sahoo, S.K. Vitamin B_6 Cofactor Derivative: A Dual Fluorescent Turn-On Sensor to Detect Zn^{2+} and CN^{-} Ions and Its Application in Live Cell Imaging. *Chem. Select* **2017**, *2*, 7570–7579. [CrossRef]
39. Jung, J.M.; Yun, D.; Lee, H.; Kim, K.-T.; Kim, C. Selective chemosensor capable of sensing both CN^{-} and Zn^{2+}: Its application to zebrafish. *Sens. Actuators B* **2019**, *297*, 126814. [CrossRef]
40. Jeong, H.Y.; Lee, S.Y.; Han, J.; Lim, M.H.; Kim, C. Thiophene and diethylaminophenol-based "turn-on" fluorescence chemosensor for detection of Al^{3+} and F^{-} in a near-perfect aqueous solution. *Tetrahedron* **2017**, *73*, 2690–2697. [CrossRef]
41. Wu, Y.; Guo, H.; James, T.D.; Zhao, J. Enantioselective Recognition of Mandelic Acid by a 3,6-Dithiophen-2-yl-9 *H* -carbazole-Based Chiral Fluorescent Bisboronic Acid Sensor. *J. Org. Chem.* **2011**, *76*, 5685–5695. [CrossRef] [PubMed]
42. Kim, Y.S.; Lee, J.J.; Lee, S.Y.; Jo, T.G.; Kim, C. A highly sensitive benzimidazole-based chemosensor for the colorimetric detection of Fe(II) and Fe(III) and the fluorometric detection of Zn(II) in aqueous media. *RSC Adv.* **2016**, *6*, 61505–61515. [CrossRef]
43. Na, Y.J.; Choi, Y.W.; Yun, J.Y.; Park, K.; Chang, P.; Kim, C. Dual-channel detection of Cu^{2+} and F^{-} with a simple Schiff-based colorimetric and fluorescent sensor. *Spectrochim. Acta A* **2014**, *136*, 1649–1657. [CrossRef] [PubMed]
44. Würth, C.; Grabolle, M.; Pauli, J.; Spieles, M.; Resch-Genger, U. Relative and absolute determination of fluorescence quantum yields of transparent samples. *Nat. Protoc.* **2013**, *8*, 1535–1550. [CrossRef] [PubMed]
45. Job, P. Formation and stability of inorganic complexes in solution. *Ann. Chim. Appl.* **1928**, *9*, 113.
46. Benesi, H.A.; Hildebrand, J.H. A Spectrophotometric Investigation of the Interaction of Iodine with Aromatic Hydrocarbons. *J. Am. Chem. Soc.* **1949**, *71*, 2703–2707. [CrossRef]
47. Lin, H.-Y.; Cheng, P.-Y.; Wan, C.-F.; Wu, A.-T. A turn-on and reversible fluorescence sensor for zinc ion. *Analyst* **2012**, *137*, 4415–4417. [CrossRef]
48. Hsieh, W.H.; Wan, C.F.; Liao, D.J.; Wu, A.T. A turn-on Schiff base fluorescence sensor for zinc ion. *Tetrahedron Lett.* **2012**, *53*, 5848–5851. [CrossRef]
49. Choi, Y.W.; You, G.R.; Lee, J.J.; Kim, C. Turn-on fluorescent chemosensor for selective detection of Zn^{2+} in an aqueous solution: Experimental and theoretical studies. *Inorg. Chem. Commun.* **2016**, *63*, 35–38. [CrossRef]
50. Purkait, R.; Mahapatra, A.D.; Chattopadhyay, D.; Sinha, C. An azine-based carbothioamide chemosensor for selective and sensitive turn-on-off sequential detection of Zn(II) and $H_2PO_4^{-}$, live cell imaging and INHIBIT logic gate. *Spectrochim. Acta A* **2019**, *207*, 164–172. [CrossRef]
51. Harrison, R.M.; Laxen, D.P.H.; Wilson, S.J. Chemical associations of lead, cadmium, copper, and zinc in street dusts and roadside soils. *Environ. Sci. Technol.* **1981**, *15*, 1378–1383. [CrossRef]
52. Tsui, Y.-K.; Devaraj, S.; Yen, Y.-P. Azo dyes featuring with nitrobenzoxadiazole (NBD) unit: A new selective chromogenic and fluorogenic sensor for cyanide ion. *Sens. Actuators B Chem.* **2012**, *161*, 510–519. [CrossRef]
53. Park, G.J.; Lee, J.J.; You, G.R.; Nguyen, L.; Noh, I.; Kim, C. A dual chemosensor for Zn^{2+} and Co^{2+} in aqueous media and living cells: Experimental and theoretical studies. *Sens. Actuators B Chem.* **2016**, *223*, 509–519. [CrossRef]
54. Park, G.J.; Na, Y.J.; Jo, H.Y.; Lee, S.A.; Kim, A.R.; Noh, I.; Kim, C. A single chemosensor for multiple analytes: Fluorogenic detection of Zn^{2+} and OAc^{-} ions in aqueous solution, and an application to bioimaging. *New J. Chem.* **2014**, *38*, 2587–2594. [CrossRef]
55. Hwang, I.H.; Choi, Y.W.; Kim, K.B.; Park, G.J.; Lee, J.J.; Nguyen, L.; Noh, I.; Kim, C. A highly selective and sensitive fluorescent turn-on Al^{3+} chemosensor in aqueous media and living cells: Experimental and theoretical studies. *New J. Chem.* **2016**, *40*, 171–178. [CrossRef]
56. Park, S.; Hong, K.H.; Hong, J.I.; Kim, H.J. Azo dye-based latent colorimetric chemodosimeter for the selective detection of cyanides in aqueous bis-tris buffer. *Sens. Actuators B* **2012**, *174*, 140–144. [CrossRef]

57. Guo, Z.; Niu, Q.; Yang, Q.; Li, T.; Chi, H. A highly selective and sensitive dual-mode sensor for colorimetric and turn-on fluorescent detection of cyanide in water, agro-products and living cells. *Anal. Chim. Acta* **2019**, *1065*, 113–123. [CrossRef]
58. Venkatesan, V.; Kumar, S.K.A.; Sahoo, S.K. Spectrophotometric and RGB performances of a new tetraphenylcyclopenta-derived Schiff base for the quantification of cyanide ions. *Anal. Methods* **2019**, *11*, 1137–1143. [CrossRef]